

Effect of Solidification Shrinkage on Topography Formation in Laser Surface Melting

Skoltech
Materials

D.V. Panov, O. A. Rogozin, O. V. Vasilyev.

Center for
Materials
Technologies

Motivation

The topography after laser surface melting is the result of a combination of different physical phenomena. Mathematical modeling can be used to estimate the effect of thermophysical properties on the resulting topography. The most important phenomena such as capillarity, thermocapillarity, evaporation are considered in a number of studies. An important but most often neglected effect is the shrinkage during solidification. In the presented work an approach modelling the effect of shrinkage on the solidification is considered and the results of numerical simulations are presented.

Mathematical model

Let us consider a domain consists of three phases such that:

$$\rho = (1 - \alpha)\rho_G + \phi\rho_L + (\alpha - \phi)\rho_S,$$

$$\rho h = (1 - \alpha)\rho_G h_G + \phi\rho_L h_L + (\alpha - \phi)\rho_S h_S,$$

where ρ_P is the density of a given phase P, h_P is the enthalpy of a given phase P, α is the volume fraction of metal and ϕ is the volume fraction of liquid metal.

The system of governing equations for α , v , h can be written as follows:

$$\begin{aligned} \frac{\partial \alpha}{\partial t} + \nabla \cdot (\alpha v) &= \nabla \cdot v, \\ \nabla \cdot v &= - \frac{(\rho_L - \rho_S) D_t \phi + \phi D_t \rho_L}{\phi \rho_L + (1 - \phi) \rho_S}, \\ \frac{\partial \rho v}{\partial t} + \nabla \cdot (\rho v \otimes v) &= - \nabla p + \underbrace{\nabla \cdot \left(- \frac{K \alpha (\alpha - \phi)^2}{\phi^2 + \epsilon} v \right)}_{\text{Brinkman penalization}} + \underbrace{\rho}_{\text{gravity}} \\ &\quad - \underbrace{\gamma (\nabla \cdot \alpha) \nabla \alpha}_{\text{surface tension}} + \underbrace{\frac{d\gamma}{dT} (\alpha \times \nabla T \times \alpha) |\nabla \alpha|}_{\text{Marangoni force}} - \underbrace{p_{\text{recoil}}(T) \nabla \alpha}_{\text{recoil pressure}}, \\ \frac{\partial \rho h}{\partial t} + \nabla \cdot (\rho v h) &= \underbrace{\nabla \cdot (k \nabla T)}_{\text{heat conductivity}} + \underbrace{I_L |\nabla \alpha|}_{\text{laser heat source}} + \underbrace{Q_{\text{evap}}(T) |\nabla \alpha|}_{\text{evaporation cooling}}. \end{aligned}$$

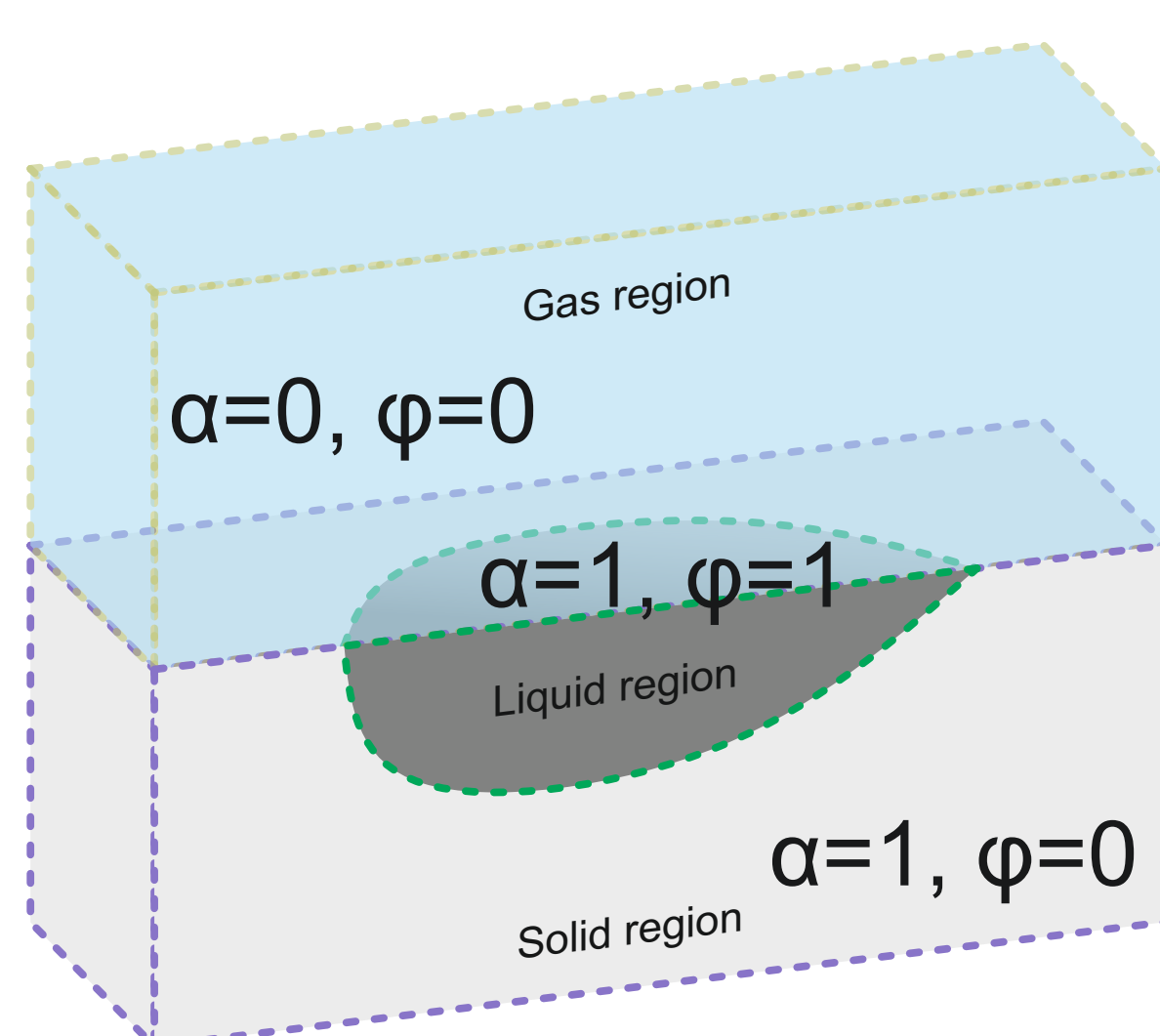


Figure 1: Schematic representation of the computational domain with the metal volume fraction α and the molten metal volume fraction ϕ distribution for different phases.

Details of the computational method and implementation:

- Finite Volume Method;
- Implicit Euler time integration;
- Volume fraction of metal α is treated with geometric Volume of Fluid method;
- Segregated solution;
- All the procedures are implemented in OpenFOAM®.

Conclusions

- An approach to incorporate metal density variability in mathematical model of melting process is presented;
- The difference in the final surface state of the considered numerical solutions shows the importance of considering the temperature compressibility of metal.

References

- [1] Pitscheneder W, DebRoy T, Mundra K and Ebner R 1996 Role of sulfur and processing variables on the temporal evolution of weld pool geometry during multikilowatt laser beam welding of steels *Weld J.* **75** 71–80

2D vertical solidification and pipe shrinkage

Thermophysical properties are taken for pure aluminum. The surface tension is taken as a constant. The rectangular domain size is $\Omega \in [0.8 \times 10^{-3} \text{ m}]^2$.

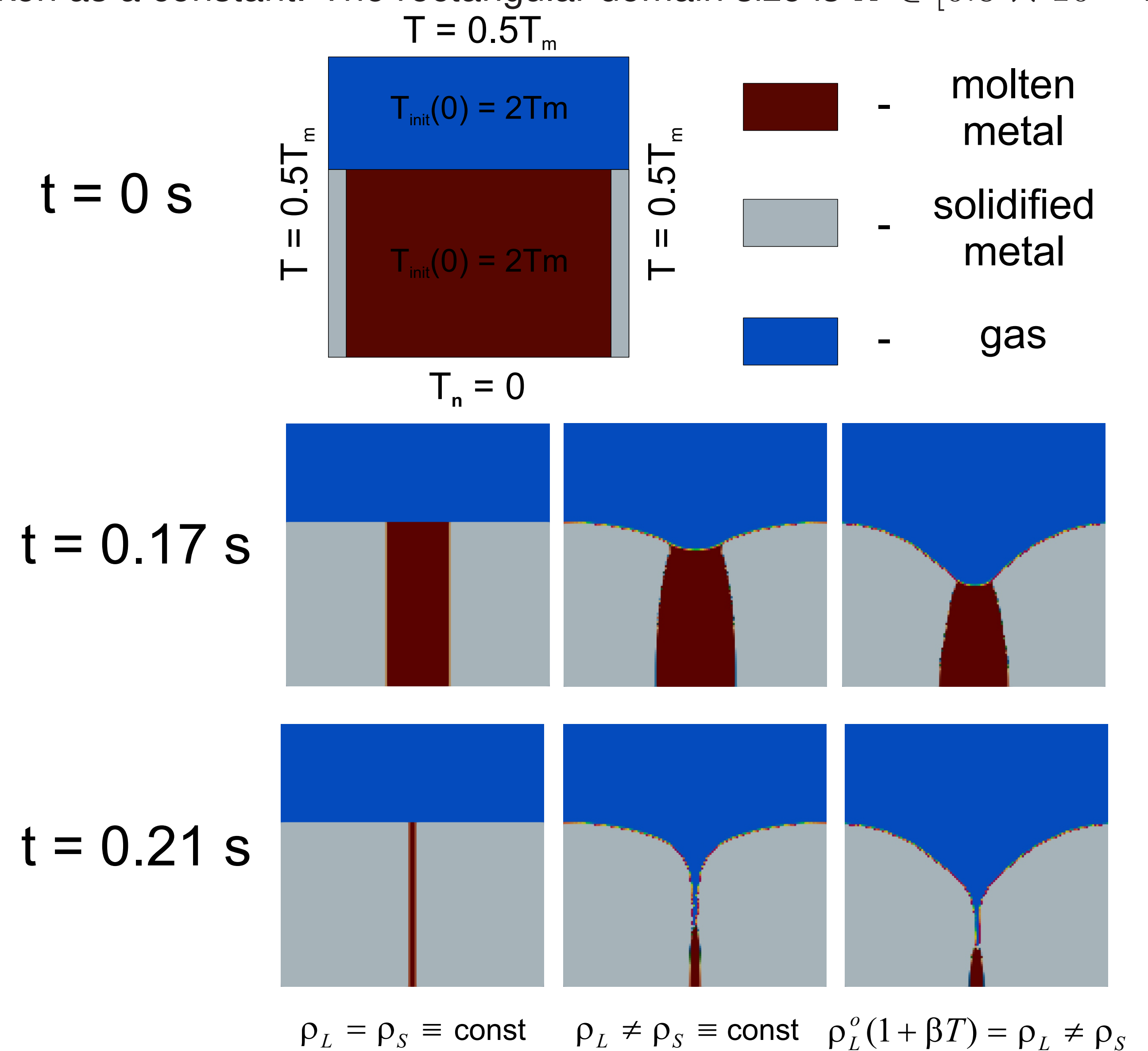


Figure 2: Aluminum vertical solidification problem and its numerical solution for phase distribution at different times for different cases of densities ρ_L and ρ_S .

In the case of a difference in density between solid and liquid phases, a kind of solidification crack develops. This phenomenon is known as “pipe shrinkage” in casting.

2D laser pulsed melting

The results of the study on mathematical modeling of pulsed laser melting by Pitscheneder et al. are used as a benchmark [1]. A top-hat CO₂ laser beam with power of 5200 W irradiates at a point for 5 seconds.

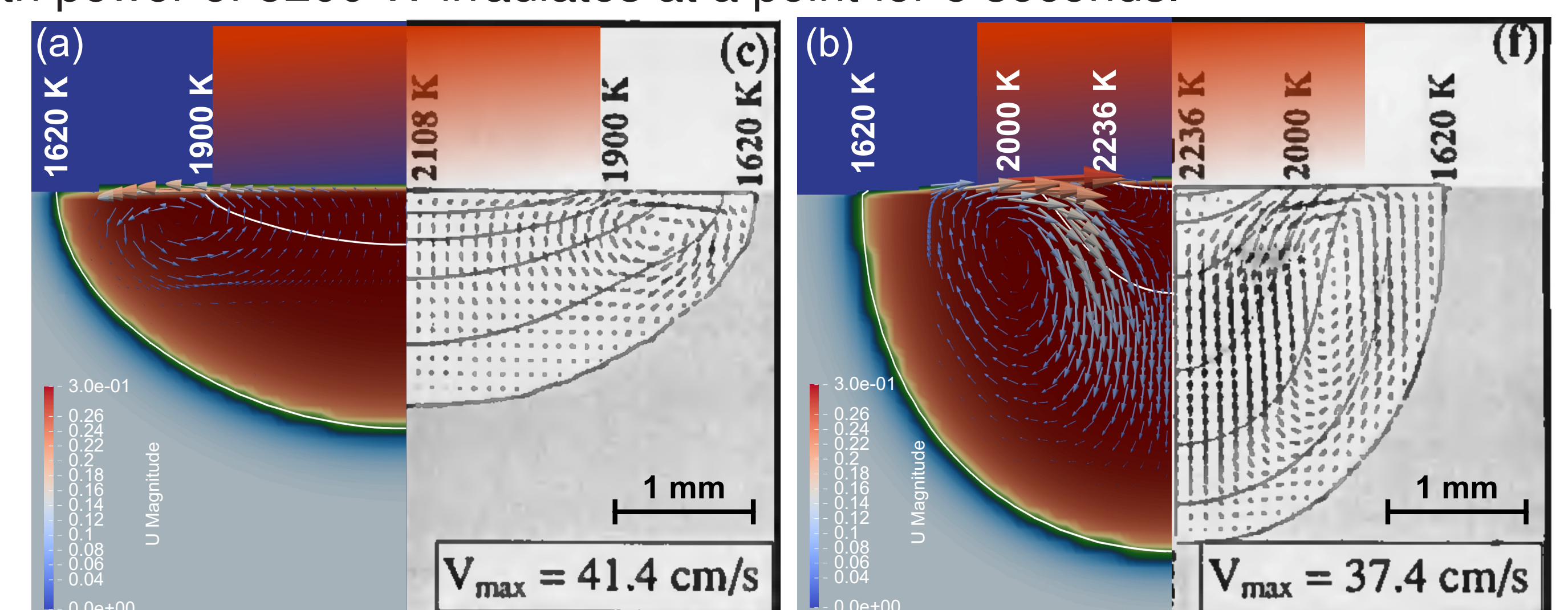


Figure 3: Comparison of numerically calculated molten metal fraction, temperature contours and velocity distribution for different sulfur concentrations of 20 ppm (a) and 150 ppm (b) in the presented work and in Pitscheneder et al. [1]

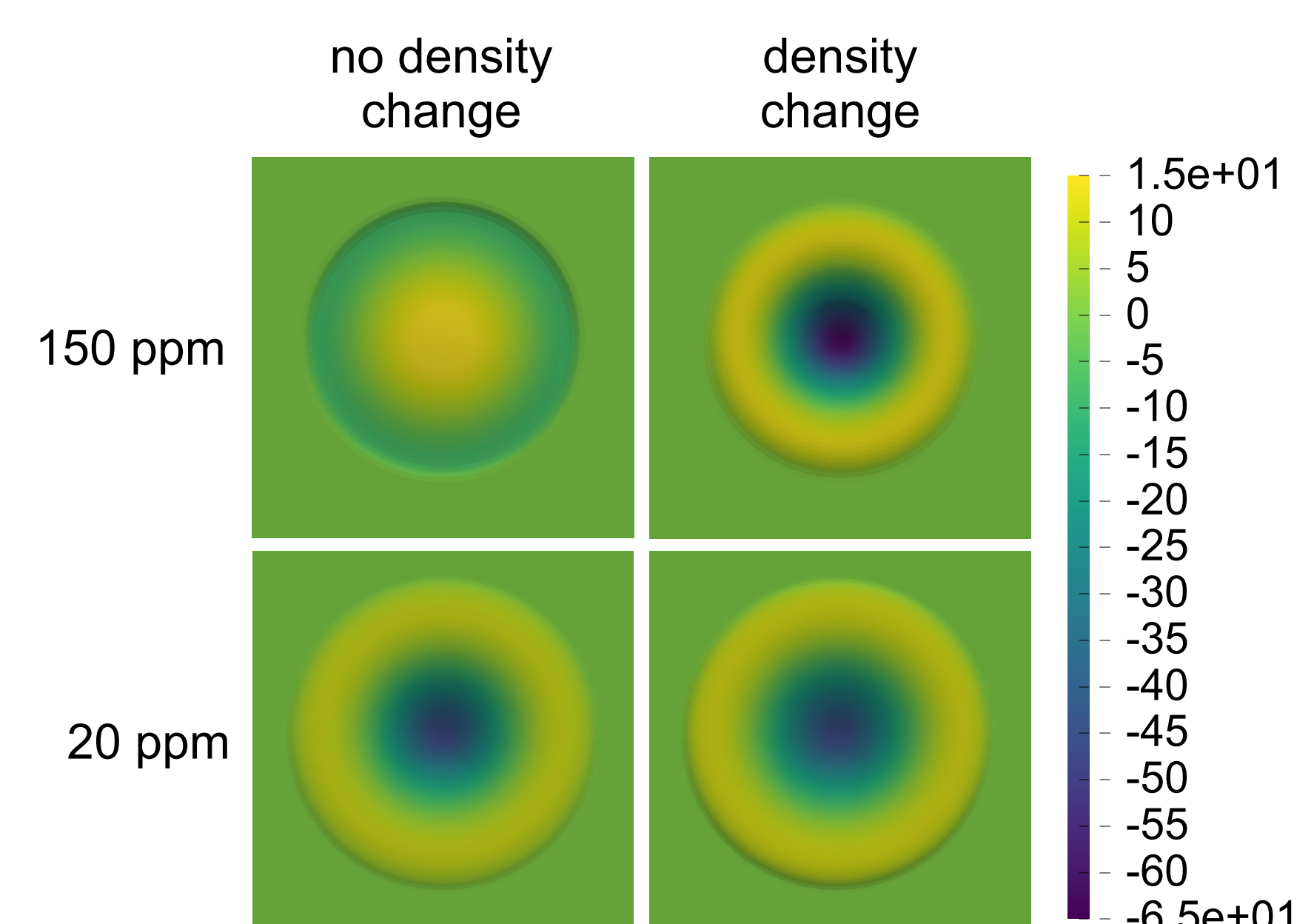


Figure 4: Numerically calculated surface topography after solidification for various sulfur concentrations in case of constant and variable density.

The final surface topography defines by Marangoni flow and solidification shrinkage.